Climate Change Initiative
Living Planet Fellowship

2014

Martin Hieronmyi

Helmholtz-Zentrum Geesthacht

4000112803/15/I-SBo

European Space Agency
Agence spatiale européenne

STANDARD COVER PAGE FOR ESA STUDY CONTRACT REPORTS

ESA STUDY CONTRACT REPORT		
ESA Contract No: 4000112803/15/I-SBo	SUBJECT: The Living Planet Fellowship "Ocean Colour at low sun and high waves (LowSun-OC)"	CONTRACTOR: Helmholtz-Zentrum Geesthacht
* ESA CR( )No:	No. of Volumes:....1 This is Volume No:....1	CONTRACTOR'S REFERENCE:

ABSTRACT:
The spectral reflectance, i.e. colour, of the water changes with sun altitude. If the sun is low above the horizon, usually more light is reflected at the surface, less light can transfer into the water, and the water body appears darker. In the presence of waves, even more light is reflected at the surface and the underwater light field gets more scattered and diffuse. Thus, sun altitude and wind-waves affect the ocean colour (OC). The objectives of the Fellowship project were (1) to study wind and wave effects on ocean surface reflectance properties, (2) to develop an ocean colour algorithm for Sentinel-3 OLCI, and finally (3) to study potential wind-effects on OC products and OC-CCI data.

The work described in this report was done under ESA Contract. Responsibility for the contents resides in the

Names of authors: Martin Hieronymi

** NAME OF ESA STUDY MANAGER: Plummer DIV: EOP-SC DIRECTORATE: EOP	ESA BUDGET HEADING: E-0073-01-L

CCI Living Planet Fellowship
Final Report

Ocean Colour at low sun and high waves (LowSun-OC)

Martin Hieronymi
Institute of Coastal Research, Helmholtz-Zentrum Geesthacht (HZG)

February 1st, 2017
(Revised June 2017)

Introduction

The spectral reflectance, i.e. colour, of the water changes with sun altitude. If the sun is low above the horizon, usually more light is reflected at the surface, less light can transfer into the water, and the water body appears darker. In the presence of waves, even more light is reflected at the surface and the underwater light field gets more scattered and diffuse. Thus, sun altitude and wind-waves affect the ocean colour (OC). The objectives of the Fellowship project were (1) to study wind and wave effects on ocean surface reflectance properties, (2) to develop an ocean colour algorithm for Sentinel-3 OLCI, and finally (3) to study potential wind-effects on OC products and OC-CCI data.

Two main achievements were delivered in the form of peer-reviewed publications. Firstly, the determination of reflectance (and transmittance) properties of ocean surfaces as function of all climatologically-relevant sea states and wind conditions and under consideration of light polarization. This is basically a revision of the classical Cox-Munk model [Cox and Munk, 1954], which is used in many radiative transfer models. Secondly, the OLCI Neural Network Swarm (ONNS) in-water algorithm was developed. The new OC algorithm uses similar approaches as the OC-CCI consortium, namely selection and blending of specific algorithms by means of fuzzy logic water type classification. Thus, the algorithm is applicable for most water types including clear oceanic, coastal and inland waters, and extreme absorbing or scattering waters. The improvement of OC product quality in Case-2 waters is an emphasis of OC-CCI. After appropriate validation (and possible fine-tuning) of the new algorithm, it is planned to make ONNS freely available via ESA's Sentinel toolbox SNAP.

Point three of the objectives, wind-effects on OC, is subject to ongoing research. Beyond wave shapes, some further impacts of wind have been identified, e.g. whitecaps, air bubbles in the water column, and mixing of the upper ocean layer. However, a comprehensive study regarding these impacts on ocean colour has not been achieved. Potential for research and development continuity of the Fellowship project is provided.

Methodological approaches

Revision of reflectance properties of ocean waves

State of the art wave modelling was applied with full consideration of sea state-dependent wave elevations and wind-related wave slope variance. The modelled wave profiles are two-dimensional in wave-propagation and -elevation direction. For the first time, non-linear wave shape effects have been considered. This is applied in order to better reflect observations of wave crest distributions and to provide more realistic wave representations. All ocean wave classes are included, ranging from capillary to swell waves. Modelled sea surfaces are representative for the various sea states that occur in the ERA-Interim global wave climatology.

Wave profiles were implemented into a newly developed ray tracing code which detects shadowing of the wave structure and allows tracing of multiple reflections at the wavy surface. After determining

of ray propagations, directional distributions, and contact points, Fresnel's equations were applied in order to calculate the polarized rates of reflected and transmitted light per angular direction. Based on this, wave effects on the light transfer are investigated for all relevant sea states and different local wind-wave regimes (e.g. for inland waters). Furthermore, effects of roughness-changes in terms of mean-square slope, *mss*, are studied. Tests for comparisons with statistical wave slope distributions have been conducted.

Radiative transfer simulations

The basis of ocean colour algorithms is radiative transfer simulations. It has been decided to decouple atmospheric and oceanic radiative effects and only develop an in-water algorithm for remote sensing retrieval of water constituents. Indeed, the in-water part is a multi-algorithm approach where homogeneous atmospheric conditions and sun-viewing geometries are expected, i.e., sun and viewing direction in zenith. An eligible atmospheric correction needs to provide these conditions to the in-water part, despite low sun, sun glint, strong wind or bubble entrainment. For the purpose of in-water algorithm development, around half a million Hydrolight simulations have been conducted using the mainframe computer of the HZG data centre. It should be noted that Hydrolight's sea surface treatment is based on the Cox-Munk model; but with sun and viewing at zenith, wind and wave effects are less significant. The results of the simulations were pooled in a database which shall be made publically available soon. The dataset covers 10^5 complete sets of inherent optical properties of water, e.g. specific absorption and scattering properties, as well as computed radiative quantities, e.g. remote sensing reflectance. The simulations cover the full visible (VIS) and near-infrared (NIR) spectral range (380:2.5:1100 nm) and in addition some short-wave infrared (SWIR) bands of Sentinel-3 SLSTR. The optical water properties cover clearest sea water as well as cases with extreme absorbing or scattering waters. Special features include differentiation of inelastic scattering processes and utilisation of chlorophyll-specific absorption spectra of different algae types. This means that there is potential for future publications.

Water type classification

In cooperation with OC-CCI and HZG colleague Dagmar Müller, the fuzzy logic water type classification scheme of Moore et al. (2001) was adopted and applied to the simulated dataset. One alteration to the original approach is the application of brightness-scaled remote sensing spectra, i.e. the spectral shape matters more than the amplitudes. The rationale behind is that for example (wind speed-related) air bubbles in water and other scattering-related effects may shift the total spectrum rather than change it spectrally (closer examination of the effects must be made). The applied classification scheme is based on 11 OLCI bands and yields differentiation into 13 optical water types (OWT). Each of the optical water types represents a typical spectral shape of the remote sensing reflectance (just above the water surface). The idea of the fuzzy logic classification scheme is to select the most appropriate ocean colour algorithms and blend their results according to specific memberships in order to gain smooth transitions and high quality data.

Ocean colour algorithm

Based on the simulations and classification scheme, 13 sets of neural networks (NN) have been trained. The overall processor contains blending of OWT and an uncertainty analysis and is called OLCI Neural Network Swarm (ONNS). The basic concept of NNs is already applied for MERIS [Doerffer and Schiller, 2007] and also in the Sentinel-3 OLCI ground segment processor of ESA for the generation of Case-2 water products [Brockmann et al., 2016]. In comparison to the previous processors, ONNS is applicable over wider scope of water constituents and delivers additional optical products, e.g. the colour code according historical Forel-Ule scale and diffuse attenuation coefficients.

In situ measurements

In the framework of Sentinel-3 Validation Team (S3VT) efforts and a research cruise on RV *Heincke*, radiometric measurements have been conducted with focus on the determination of the surface reflectance factor. This factor is used to determine the spectral remote sensing reflectance from above-water measurements of the downwelling irradiance, sky radiance, and surface (upwelling) radiance. Thus, measurements of depth profiles of the light field, directly beneath the surface, and above-water (under different sun-viewing angles) have been carried out. In addition to radiometric measurements, numerous optical parameters, e.g. chlorophyll-specific absorptions and volume scattering functions, as well as concentrations of water constituents have been measured on board RV *Heincke*. The analysis of the data is not yet completed. A planned campaign in the high latitudes (Arctic) on board RV *Polarstern* was rescheduled for May-June 2017. The collected data will be used to verify the theoretical findings regarding surface reflectance properties. Furthermore, the data serve the validation of the new ocean colour algorithm ONNS.

Results and discussion

Polarized reflectance and transmittance distribution functions of the ocean surface

It is found that reflectance and transmittance distribution functions, *RDF* and *TDF*, primarily depend on the mean-square slope of modelled sea surfaces; a better and more distinct relationship as compared to the related wind speed, significant wave height, mean wave period, or steepness of the sea state can be provided. Figure 1 shows the angular distribution (in viewing angles ϑ_v) for light incidence from individual directions. A perfectly flat sea surface, where *mss* = 0, reflects the incident light beam directly and solely into the direction with negative incidence angle (Figure 1a-d). If the surface roughens, fractions of reflected light shift into directions alongside the main reflection axis. As soon as the roughness increases, the affected angular range expands and reflection/transmission rates redistribute, i.e. are getting smaller. Very high *mss*, i.e. heavy seas, causes reflections of light into the entire upper hemisphere; nearly a uniform distribution or Lambertian surface (Fig. 1a). The directional distributions shift with increasing incidence angle ϑ_i. Interestingly, in case of $\vartheta_i = 60°$, the direction of highest reflection rates changes with increasing roughness towards larger reflection angles (Fig. 1c). In case of $\vartheta_i = 85°$, the maximum moves from $\vartheta_v = -85°$ at low *mss* to -70° at highest *mss* (Fig. 1d). The redistribution of reflected fractions due to multiple scattering at the surface impacts the *RDF*, also in terms of total reflectance. Furthermore, Figure 1d illustrates the increasing shadowing of reflection directions very near the horizon (< -85°) with higher seas. Regarding *TDF*, the directional distribution is much narrower (Fig. 1e-h) and a small spread of the affected angle range can be observed for increasing incidence angles. Near the horizon however, the right side of the distribution function (towards zero) is blocked due to wave shadowing (Fig. 1h).

The principle correlation of mean-square slope and wind speed is known and already used for a long time, e.g. Cox and Munk [1954]. But using slope statistics loses sight of the large-scale wave structure, which governs shadowing of incident light as well as shielding and redistribution of reflection directions near the horizon. The sea state steepness increases with surface roughness too and is an important factor controlling multiple reflections at the surface. A high degree of accuracy for redistribution of reflectance fractions from multiple reflections can only be achieved by using fully shaped surfaces; it cannot be accomplished with random and unrelated wave slopes according a slope distribution. Multiple scattering originates mainly at the backside of steep wave crests, whereby free path lengths to the next reflection points are mostly short, within some centimetres. Indeed, it makes a difference where steep slopes are located. The net effect of multiple reflections is to redistribute reflectance and transmittance fractions in the respective hemispheres and to slightly increase the net transmission of light into the sea – this relates to large light incidence angles, mostly > 60°. In principle this means that slope distributions, i.e., the Cox-Munk model, provide similar

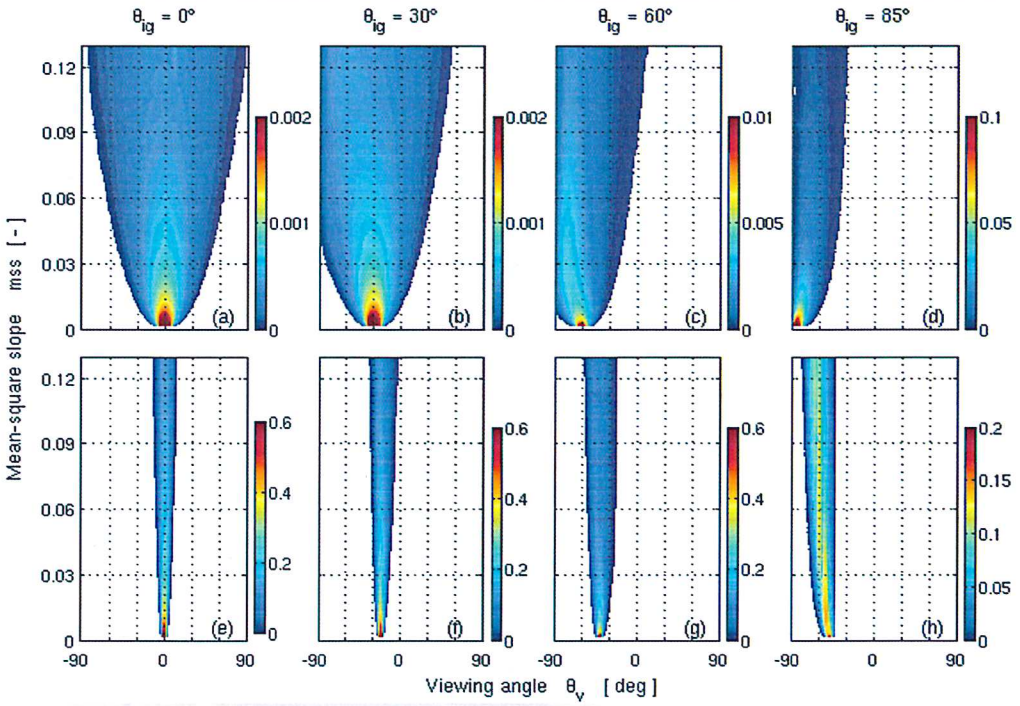

Figure 1: RDF (top) and TDF (bottom) as function of mean-square slopes of all sea states and different light incidence angles. White corresponds to zero (from Hieronymi [2016]).

results for small light incidence angles, e.g., < 45°, because multiple reflections basically play no role; with increasing incidence angles and depending on roughness, significant deviations can occur. However, an overall assessment of shadowing and multiple reflections yields lower net transmission in comparison to previous studies [Preisendorfer and Mobley, 1986], i.e., on average this study yields somewhat higher reflectance values with implications to energy flux and heating rates, but there is high variability related to sea states. In many sea regions, significant wave height and mean wave period seem to be better indicators of surface roughness and therefore reflectance properties.

RDF (ϑ_{ig}, ϑ_v) and *TDF* (ϑ_{ig}, ϑ_v) parallel and perpendicular to the plane of incidence are provided in the form of look-up-tables as function of the mean-square slope of the sea surface and are related to other sea state parameters. An example is provided in Fig. 2. *mss* is a measure for the roughness of the sea, but also a measure of the degree of the nonlinearity of transport processes, such as gas transport. The *mss*-related reflectance and transmittance functions can be used for a large variety of sea states and wind speeds as up/down-wind and cross-wind properties of the sea surface. By means of the data with high angular resolution, irradiance and radiance reflectances can be computed using desired environmental conditions, i.e., sky radiance distributions from clear or cloudy skies. The data provided should be implemented into vector radiative transfer models of the coupled atmosphere-ocean system.

A detailed discussion of the findings with link to *RDF* and *TDF* datasets is published in: Hieronymi (2016) "Polarized reflectance and transmittance distribution functions of the ocean surface", *Optics Express*, 24 (14). Additional information and specific questions have been addressed in an additional conference paper: Hieronymi (2016) "Reflectance and transmittance properties of sea surfaces – Aspects of polarized ray tracing", Proceedings of the *Living Planet Symposium*.

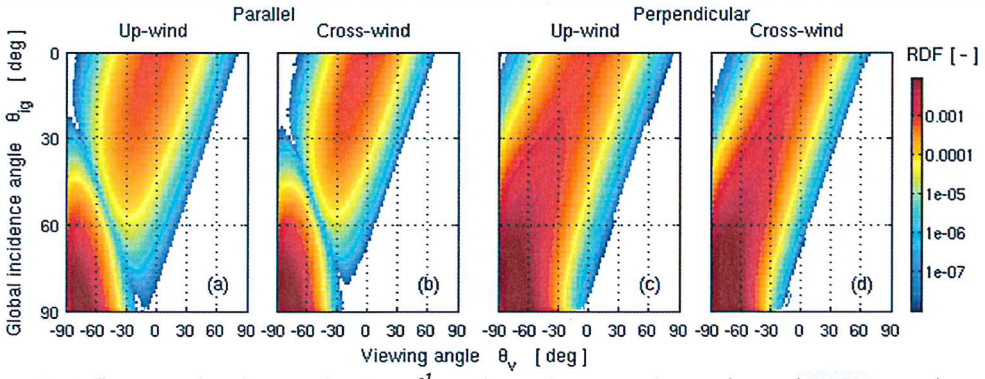

Figure 2: Reflectance distributions for 10 m s^{-1} wind speed separated according polarization mode and wind direction components (logarithmic colour scale; from Hieronymi [2016]).

OLCI Neural Network Swarm (ONNS) – ocean colour algorithm for open ocean and coastal waters

Totally independent from the surface reflectance work, an in-water ocean colour algorithm has been developed. It has been decided that it is more convenient to include wind and wave related effects to the atmospheric correction (AC) or possibly to a separate "air-sea interface correction". Therefore the new algorithm, ONNS, is based on fully normalized remote sensing reflectances and assumes a clear maritime atmosphere and moderate wind speed of 5 m s^{-1} (global mean). Many in-water algorithms are based on fully normalized R_{rs}, where viewing and sun zenith angles are perpendicular. For example, fully normalized data from different sensors are merged for the OC-CCI dataset. It is duty of the AC to provide reliable normalized R_{rs} using sun-viewing geometry, sea state information, and possibly to account for wind-related effects such as air bubbles, whitecaps, and sea spray. For the purpose of ONNS development, two AC processors were examined more closely, namely Polymer [Steinmetz et al., 2011] and C2RCC [Brockmann et al., 2016]. The latter, C2RCC, is freely available via SNAP and delivers (compared to the expectation) plausible and usable spectral reflectance shapes as input for the new in-water algorithm. C2RCC is therefore used here for atmospheric correction.

We selected 11 (out of 21) OLCI wavebands for NN input (namely at 400, 412.5, 442.5, 490, 510, 560, 620, 665, 755, 777.5, and 865 nm). Wavebands that are affected by phytoplankton fluorescence (at 673.75, 681.25, and to only a minor degree at 708.75 nm) are not utilized, since the fluorescence quantum yield efficiency and therefore peak height is quite variable (also with respect to AC) and usage of the fluorescence line height does not necessarily increase the retrieval performance. The main purpose of other OLCI NIR bands is atmospheric correction, e.g., due to oxygen and water vapour absorption and optical features of aerosols. Thus, satellite-derived R_{rs} is not provided for all of the NIR bands [Steinmetz et al., 2011]. Further discussion on the ONNS design is provided in Hieronymi et al. [2017]. The selected output parameters are mostly common ocean colour products:

(1) Concentration of chlorophyll, *Chl* [mg m^{-3}],
(2) Concentration of inorganic suspended matter (minerals), *ISM* [g m^{-3}],
(3) Absorption coefficient of CDOM at 440 nm, $a_{cdom}(440)$ [m^{-1}],
(4) Absorption coefficient of phytoplankton particles at 440 nm, $a_p(440)$ [m^{-1}],
(5) Absorption coefficient of minerals at 440 nm, $a_m(440)$ [m^{-1}],
(6) Absorption coefficient of detritus plus gelbstoff at 412 nm, $a_{dg}(412)$ [m^{-1}],
(7) Scattering coefficient of phytoplankton particles at 440 nm, $b_p(440)$ [m^{-1}],
(8) Scattering coefficient of minerals at 440 nm, $b_m(440)$ [m^{-1}],
(9) Total backscattering coefficient of all particles (organic and inorganic) at 510 nm, $b_{bp}(510)$ [m^{-1}],
(10) Downwelling diffuse attenuation coefficient at 490 nm, $K_d(490)$ [m^{-1}],
(11) Upwelling diffuse attenuation coefficient at 490 nm, $K_u(490)$ [m^{-1}], and
(12) Forel-Ule number, *FU* [-].

Concentrations can be directly derived with NNs or alternatively, they can be estimated using IOPs, e.g., *Chl* from $a_p(440)$ or *ISM* from $b_m(440)$ [3]. The latter approach allows better adaptation of empirical relationships by means of in situ match-up data. All absorption and scattering contributions are retrieved at the reference wavelength 440 nm (pure water IOPs are known). Thereby, it is possible to estimate the total absorption, total scattering, and total attenuation coefficients. Mineral particles have usually lower absorption characteristics than CDOM, but shape-wise both are very similar. Following this reasoning, semi-analytical models, designed to retrieve IOPs from satellite data, often combine absorption by detritus (in this work only inorganic fraction) and *gelbstoff* (all water constituents which pass a filter pore size of 0.2 µm, which is often synonymous with CDOM). A similar idea holds true for the backscattering parameter. It is usually the backscattering coefficient of all marine particles together, which is measured in the field. The diffuse attenuation coefficients are used to describe the attenuation of irradiance as a function of depth in water. It can be used to compute the depth of the euphotic zone. The selection of different reference wavelengths for various parameters at 412, 440, 490, and 510 nm has to do with previous model parameterisations, historical notations, and measurement techniques; it serves for the continuous development of homogeneous datasets. The Forel-Ule colour scale was used for natural water classification long before the satellite era. In open ocean regions, the FU number is closely related to chlorophyll concentration. Thus, the index can support ocean colour trend analysis in the pre-satellite age and afterwards [Wernand et al., 2013] – also with respect to the OC Climate Change Initiative.

A subsequent set of neural nets serves to evaluate the divergence of final OC products from the original training basis, i.e., Hydrolight simulations. All NNs per water class were reapplied to their training datasets to estimate the OC products. The uncertainty nets compare the estimated value, X_E, with the initial training value, X_T. The uncertainty per product is given as approximation error:

$$\varepsilon = 100 \frac{X_E - X_T}{X_T}.$$

As it is the case for all OC products, the final approximation error is a weighted sum of the retrievals of all class-specific uncertainty NNs.

Examples of ONNS (current version 0.4) application on a Sentinel-3 OLCI scene are shown in Fig 3 and 4. Clouds, land, and inland waters are masked out (white and grey). The Baltic Sea is generally known for higher CDOM concentration compared to the open sea, i.e., more absorbing waters, whereas the Wadden Sea along the Dutch and German North Sea coast contains a lot of suspended sediment, i.e., these are scattering waters. The water type classification expresses these features. In addition, the true colour impression on the basis of the Forel-Ule scale confirms regional expectations.

Directly retrieved chlorophyll and inorganic suspended matter concentrations, as well as CDOM absorption at 440 nm, together with their accompanied uncertainty estimates, are shown in Fig. 4. All in all, the ranges of concentrations are reasonable. Previous match-up analyses showed that most of the measured Baltic *Chl* values range between ~1 and 10 mg m^{-3} with somewhat smaller values in the transition region between North and Baltic Sea in comparison with the Central Baltic Sea [e.g., Pitarch et al., 2016]. The ONNS-retrieved *Chl* values are in this range and reflect the geographic expectations. But from the filamentous patterns it can be assumed that an intense cyanobacteria bloom (possibly including floating vegetation) has developed in the Central Baltic, but the estimated biomass concentration seems too low. Whereas the portion of inorganic suspended matter in this areas seems too high. A detailed discussion on the OC products is delivered in Hieronymi et al. [2017]. Possible inclusion of flags in the overall processor, e.g. for floating material, and a proper validation of the algorithm remain to be done.

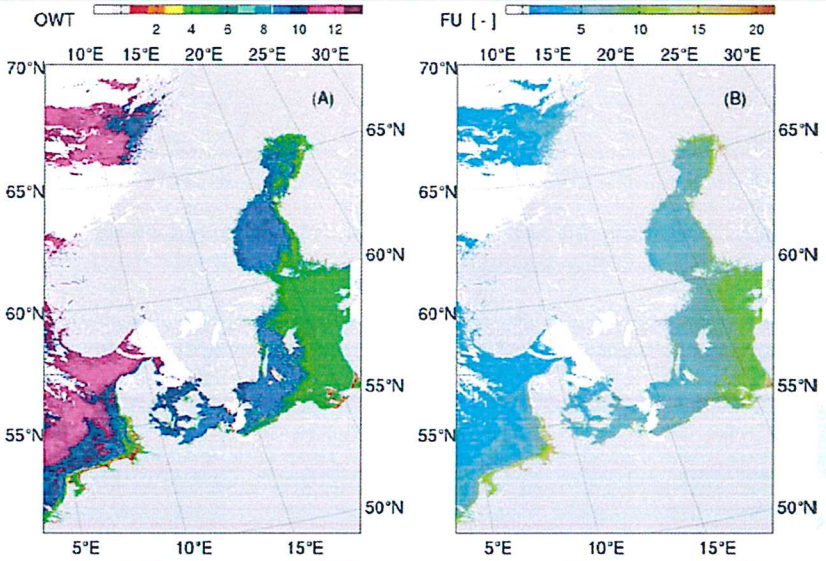

Figure 3: ONNS application to Sentinel-3 OLCI scene (2016-07-20) [contains modified Copernicus Sentinel data [2016] processed by ESA/EUMETSAT/HZG]. A: Optical water type classes with maximum membership. B: Retrieved Forel-Ule colours (from Hieronymi et al. [2017]).

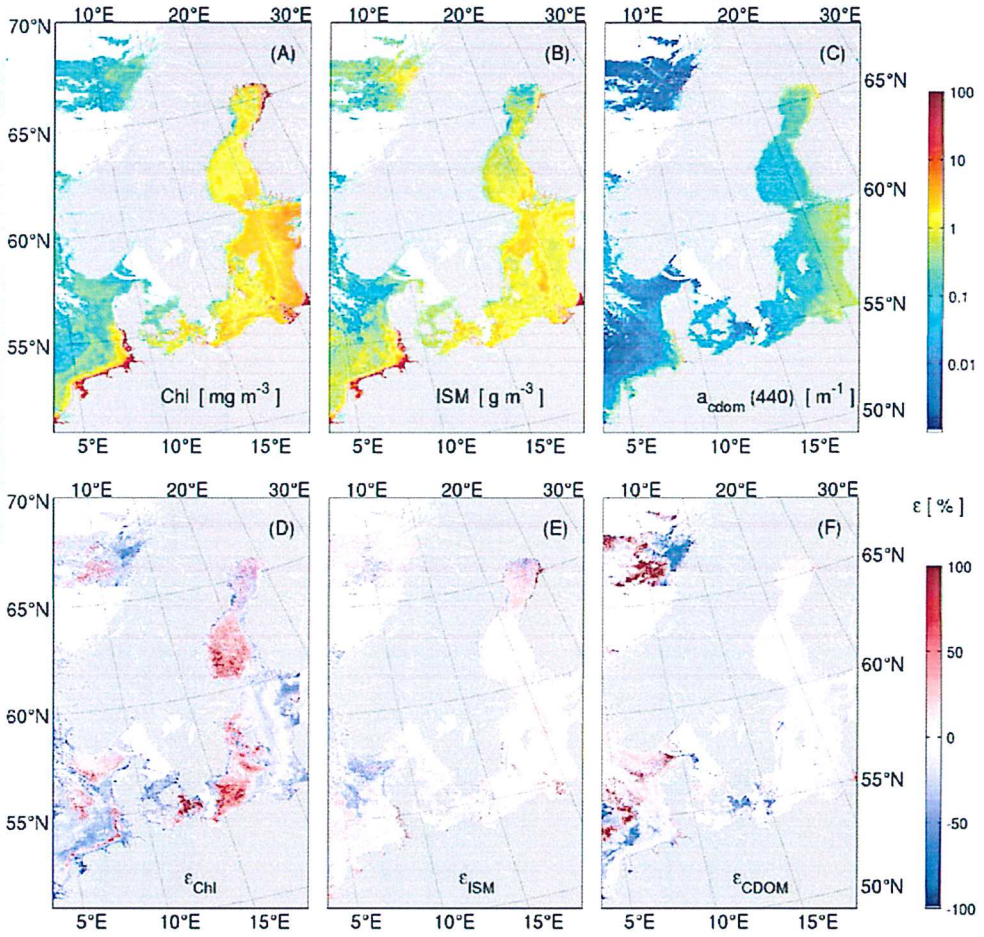

Figure 4: ONNS application to OLCI scene (2016-07-20). Top: Retrieved Chl, ISM, and CDOM. Bottom: Corresponding uncertainties (from Hieronymi et al. [2017]).

It should be noted, that the OC processor ONNS can be applied to in situ measurements as well. In this case, an atmospheric correction is not applicable. From above-water measurements, R_{rs} is determined using a surface reflectance factor, which is usually between 2 and 5 % for optimal viewing angles. The factor determines the shape of R_{rs} mainly in the violet-blue range. Thus, there are some uncertainties for the application of the classification scheme and the overall processor. Optimally, the measured R_{rs} is adapted to the input criteria for ONNS, i.e., fully normalized, a moderate wind speed, no micro-bubbles in water, etc. For testing we applied ONNS to our R_{rs} measurements on board a ferry from Cuxhaven to Helgoland in the German Bight (same day as Fig. 3 and 4). All measured spectra exhibit maximum membership in OWT 5, the same as derived from the OLCI image for the transect (Figure 3A). The results are entirely in the same magnitudes as our previous measurements in this area. ONNS estimates *Chl* along the transect between 1.7 and 4.5 mg m^{-3}, *ISM* from 0.7 to 3.4 g m^{-3}, and CDOM absorption (at 440 nm) between 0.38 to 0.68 m^{-1}. Due to tides and hydrologic changes of the Elbe river plume, *ISM* can be higher than 10 g m^{-3} near the coast.

Problems faced

In the end, the project took a different direction than planned. Although all of the four topics from the working plan were tackled, some of the points still need further investigation. From the originally planned publications, only the first is achieved. Air bubbles in water, whitecaps and the wave effects on the upwelling light field are more complex and influential than expected. In addition, the ray tracing simulations were much more time consuming and extensive than expected (despite usage of a supercomputer). Regarding the proposed "regional algorithm for high latitudes", it has been decided to not only focus on specific regions or high latitudes and instead make the algorithm applicable for all waters, including clear sea waters, extreme coastal waters, and high latitudes (many regions in high latitudes contain extreme waters, e.g. the Lena Delta is considered to be an more absorbing sea area). The new algorithm has great potential for real future use. This is more of interest for the OC-CCI and it generated synergy with the OC-CCI related extreme Case-2 water project. However, wind and wave information are not input of the current version of the in-water algorithm ONNS. It is planned to further investigate this topic and implement findings into a framework of atmospheric correction with ONNS. Another problem was that the planned cruise on board RV *Polarstern* was rescheduled for 2017. Thus, relevant in situ measurements are not yet available. In principle, ONNS should be validated for all optical water types, but in situ data (also from compiled datasets as provided by OC-CCI) are partly not suitable or available. The validation work will be continued too.

Outlook and potential R&D continuity

The interlinkage of properties of the air-sea interface with remote sensing holds great potential. One aspect is the scientific utilisation of polarization for ocean colour purposes as well as for remote sensing of aerosols or wind speed, e.g. the latter through the depolarization of whitecaps. In the last few years, polarization was implemented into some atmosphere-ocean radiative transfer codes. The implementation of the new polarized reflectance properties of sea surfaces into radiative transfer models, and therefore implicit into the ONNS algorithm and its re-evaluation, is the next logical step and will be done in the next years (depending on funding and projects).

The obvious link for project continuity is the inclusion of surface properties from climatologies or other remote sensing sources. ERA-Interim data of the ECMWF fulfil the necessary requirements. Figure 5 illustrates examples of ERA-Interim data of Europe on the same day as the above OLCI scene. The smallest resolution is on a 0.125 x 0.125° grid (OC-CCI data are delivered with 4 x 4 km resolution; unification, e.g. with 0.125° resolution of OC-CCI data, would be desirable). To make use of the new reflectance data, one needs the relative

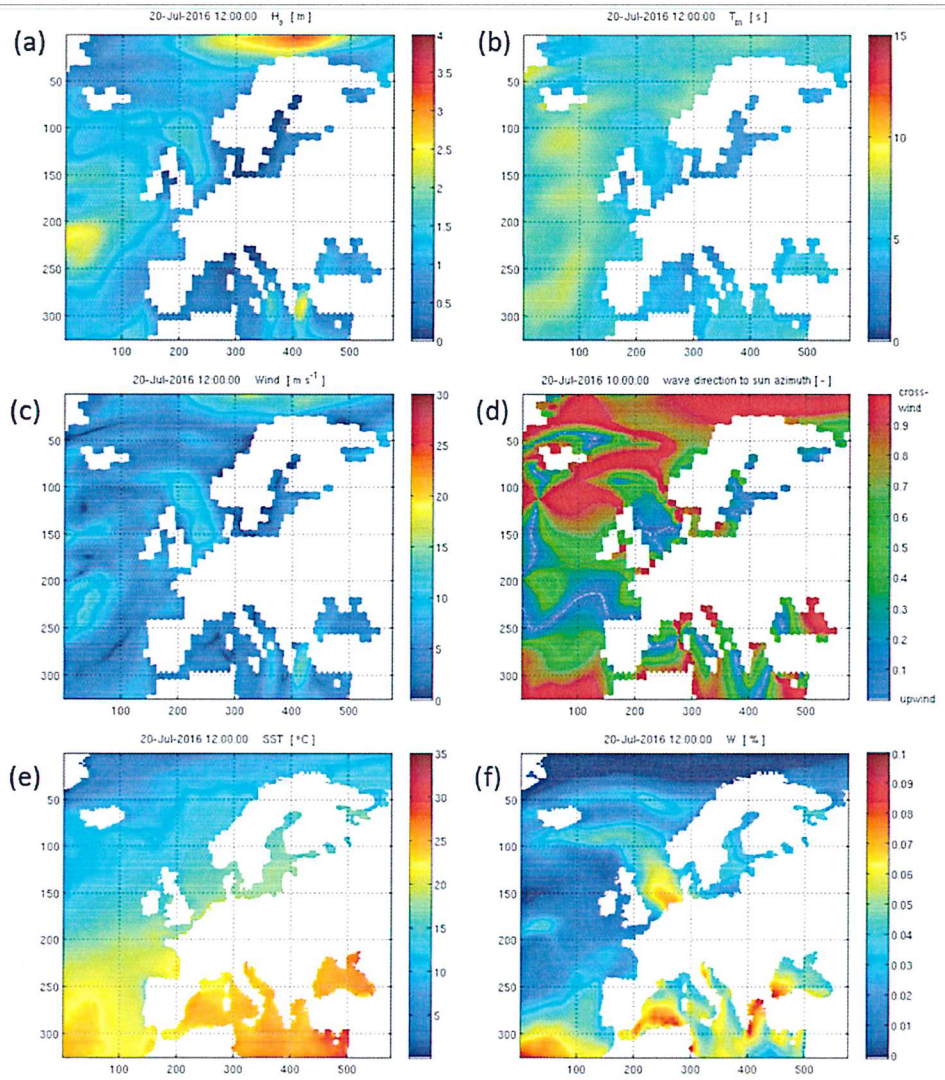

Figure 5: ERA-Interim climatological data for 2016-07-20 with 0.125° x 0.125° grid: (a) significant wave height, (b) mean wave period, (c) wind speed, and (e) sea surface temperature. (d) shows the wave direction relative to the sun position and (f) shows the corresponding oceanic whitecap fraction according Albert et al. [9] (related to satellite based wind data for 10 GHz).

angle of wave direction and sun azimuth (Fig. 5d) and in addition sea state describing data such as the mean-square slope *mss* of waves. Alternatively to the latter parameter, significant wave height H_s, mean wave period T_m, and wind speed can be deployed (from ship observations too, where *mss* is normally not directly measured). Moreover, climatological (ERA) or observed (SST_CCI) data of the sea surface temperature *SST* and corresponding wind speed allow estimation of the oceanic whitecap fraction with related sea spray aerosol emissions [Albert et al., 2015]. A sensitivity analysis could help identifying the degree of parameter influence on satellite retrieval capabilities (not only in view of ocean colour). Where appropriate, these parameters should be taken into account in ocean-atmosphere radiative transfer models, atmospheric corrections, and for OC algorithms (or possibly, in the form of an "air-sea interface correction").

First preliminary tests indicate that patterns of sea surface roughness could still be visible after atmospheric correction (here the latest C2RCC AC version 0.15 is used). Up to now, surface roughness (or wind speed) is not considered in atmospheric corrections. In this regard, sun glint removal is a

known problem too. In case of C2RCC, only the relative sun-viewing angle is used, which indirectly corrects for a mean sun glint pattern (likely corresponding to a reasonable 5 m s^{-1} wind speed). There is potential for improvement. Figure 6 illustrates the mean-square slope from the ERA-Interim climatology and localises the mentioned Sentinel-3 OLCI view. By chance, the increased wind-related roughness in the eastern Baltic Sea partly coincides with OLCI's sun glint geometry. However, it is still not clear how the roughness (possibly) transfers to the determination of optical water types (compare with Fig. 3A). The selected OLCI scene is suboptimal for quantitative tests, since significant east-west gradients of different parameters like CDOM absorption are expected in this region. The roughness pattern does not affect equally all ONNS products, but in CDOM absorption is does. Up to now, this is not considered in the delivered CDOM uncertainty product of ONNS. The present uncertainty product only refers to the deviation of the OC retrieval from its original training basis. Generally, regional features (like intertidal zones), atmospheric conditions (sub-visible clouds and other flags), and parameters from the ERA list should be included in future uncertainty estimates.

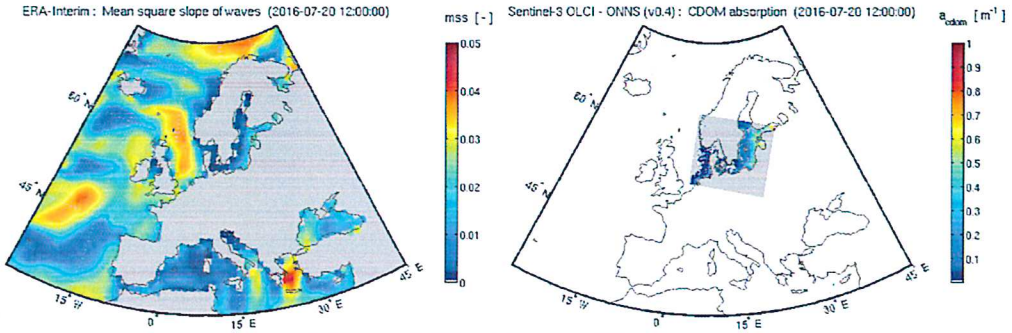

Figure 6: More than coincidence? The surface roughness (left) mirrors in the AC-corrected reflectance signal and therefore may have an effect on some OC products, e.g., CDOM absorption (right).

References

[1] Cox, C., and W. Munk (1954): Measurement of the roughness of the sea surface from photographs of the sun's glitter. *JOSA*, 44 (11), 838-850.

[2] Moore, T. S., J. W. Campbell, and H. Feng (2001): A fuzzy logic classification scheme for selecting and blending satellite ocean color algorithms. IEEE Trans. Geosci. Rem. Sens., 39(8), 1764-1776.

[3] Doerffer, R., and H. Schiller (2007): The MERIS Case 2 water algorithm. Int. J. Rem. Sens. 28(3-4), 517-535.

[4] Brockmann, C., R. Doerffer, M. Peters, K. Stelzer, S. Embacher, and A. Ruescas (2016): Evolution of the C2RCC neural network for Sentinel 2 and 3 for the retrieval of ocean colour products in normal and extreme optically complex waters. In Proc. "Living Planet Symposium", ESA SP-740.

[5] Preisendorfer, R. W., and C. D. Mobley (1986): Albedos and glitter patterns of a wind-roughened Sea surface, J. Phys. Oceanogr. 16, 1293-1316.

[6] Steinmetz, F., P. Y. Deschamps, and D. Ramon (2011): Atmospheric correction in presence of sun glint: application to MERIS. Opt. Express, 19(10), 9783-9800.

[7] Wernand, M. R., H. J. van der Woerd, and W. W. Gieskes (2013): Trends in ocean colour and chlorophyll concentration from 1889 to 2000, worldwide. PLOS one 8 (6), e63766.

[8] Pitarch, J., G. Volpe, S. Colella, H. Krasemann, and R. Santoleri (2016): Remote sensing of chlorophyll in the Baltic Sea at basin scale from 1997 to 2012 using merged multi-sensor data. Ocean Sci. 12 (2), 379-389.

[9] Albert, M. F. M. A., M. D. Anguelova, A. M. M. Manders, M. Schaap, and G. de Leeuw (2015): Parameterization of oceanic whitecap fraction based on satellite observations. ACPD, 15, 21219-21269.

Appendix – Full list of Fellowship related publications and outreach

Peer-reviewed publications

[1] Hieronymi, M., D. Müller, and R. Doerffer (2017): OLCI Neural Network Swarm (ONNS) – Ocean Color Algorithm for Open Ocean and Coastal Waters, *Frontiers in Marine Sciences, 4, 140,* doi: 10.3389/fmars.2017.00140.

[2] Hieronymi, M. (2016): Polarized reflectance and transmittance distribution functions of the ocean surface, *Optics Express*, 24 (14), pp. A1045-A1068, doi: 10.1364/OE.24.0A1045.

[3] Xi, H., M. Hieronymi, R. Röttgers, H. Krasemann, and Z. Qiu (2015): Hyperspectral Differentiation of Phytoplankton Taxonomic Groups: A Comparison between Using Remote Sensing Reflectance and Absorption Spectra, *Remote Sensing*, 7 (11), 14781-14805, doi: 10.3390/rs71114781.

Conference paper

[1] Hieronymi, M. (2016): Reflectance and transmittance properties of sea surfaces – Aspects of polarized ray tracing, Proceedings of the *Living Planet Symposium*, 9-13 May 2016, Prague, Czech Republic, ESA SP-740.

[2] Hieronymi, M., H. Krasemann, D. Müller, C. Brockmann, A. Ruescas, K. Stelzer, B. Nechad, K. Ruddick, S. Simis, G. Tilstone, F. Steinmetz, and P. Regner (2016): Ocean Colour Remote Sensing of Extreme Case-2 Waters, Proceedings of the *Living Planet Symposium*, 9-13 May 2016, Prague, Czech Republic, ESA SP-740.

[3] Hieronymi, M. (2015): Ocean Colour at Low Sun and High Waves, Proceedings of the *Sentinel-3 for Science Workshop*, ESA SP-734.

[4] Hieronymi, M., D. Müller, H. Krasemann, W. Schönfeld, R. Röttgers, and R. Doerffer (2015): Regional ocean colour remote sensing algorithm for the Baltic Sea, Proceedings of the *Sentinel-3 for Science Workshop*, ESA SP-734.

Talks

[1] Hieronymi, M., H. Krasemann, D. Müller, C. Brockmann, A. Ruescas, K. Stelzer, B. Nechad, K. Ruddick, S. Simis, G. Tilstone, F. Steinmetz, and P. Regner (2016): Ocean Colour Remote Sensing of Extreme Case-2 Waters, *Ocean Optics Conference*, 24-28 October 2016, Victoria, BC, Canada.

[2] Hieronymi, M., et al. (2016): Sentinel validation in the German Bight, *Inland-water Workshop* at HZG, 26 September 2016, Geesthacht, Germany.

[3] Hieronymi, M., H. Krasemann, D. Müller, C. Brockmann, A. Ruescas, K. Stelzer, B. Nechad, K. Ruddick, S. Simis, G. Tilstone, F. Steinmetz, and P. Regner (2016): Ocean Colour Remote Sensing of Extreme Case-2 Waters, *Living Planet Symposium*, 9-13 May 2016, Prague, Czech Republic.

[4] Hieronymi, M. (2016): Reflectance and transmittance properties of sea surfaces as function of sea state and wind speed, *International Radiation Symposium* IRS, 16.-22.04.2016, Auckland, New Zealand.

[5] Hieronymi, M. (2016): Light-water interactions at the dynamic air-sea interface, *IFK Seminar*, 02/03/2016, Geesthacht, Germany.

[6] Hieronymi, M. (2015): Solar energy transfer across the dynamic air-sea interface, *PACES II Workshop*, 27/05/2015, Geesthacht, Germany.

[7] Hieronymi, M. (2015): The Colourbar of the Sea – Validation of Remote Sensing and Optical Models, *4th EnMAP School*, 26/03/2015, Lauenburg, Germany.

Poster

[1] Hieronymi, M., D. Müller, and H. Krasemann (2016): Alternative OLCI Coastal Water Algorithm, *Colour and Light in the Ocean from Earth Observation (CLEO) Workshop*, 6-8 September 2016, ESRIN, Frascati, Italy.

[2] Hieronymi, M. (2016): Reflectance and transmittance properties of sea surfaces – Aspects of polarized ray tracing, *Living Planet Symposium*, 9-13 May 2016, Prague, Czech Republic.

[3] Hieronymi, M. (2015): Solar radiative transfer across the dynamic air-sea interface, *SOLAS Open Science Conference*, 07-11 September 2015, Kiel, Germany.

[4] Hieronymi, M. (2015): Ocean Colour at Low Sun and High Waves, *6th CCI – Collocation Meeting*, 28/09 – 01/10/2015, ESRIN, Frascati, Italy.

[5] Hieronymi, M. (2015): Ocean Colour at Low Sun and High Waves, *Sentinel-3 for Science Workshop*, 02-05 June 2015, Venice, Italy.

[6] Hieronymi, M., D. Müller, H. Krasemann, W. Schönfeld, R. Röttgers, and R. Doerffer (2015): Regional ocean colour remote sensing algorithm for the Baltic Sea, *Sentinel-3 for Science Workshop*, 02-05 June 2015, Venice, Italy.